

## Supporting Information

### **Oxygen-Bridged Triarylboryl Substituted Anthracene Emitters with High-Lying Triplet–Singlet Intersystem Crossing for Efficient deep-blue OLEDs**

Ziquan Lu<sup>a</sup>, Dehua Hu<sup>a,b,\*</sup>, Si-Wei Chen<sup>a</sup>, Ruicheng Wang<sup>a</sup>, Longjiang Xing<sup>a</sup>, Yihong Zhu<sup>a</sup>, Jieying Lin<sup>a</sup>, Yanping Huo<sup>a,b</sup>, Shaomin Ji<sup>a,b,\*</sup>

<sup>a</sup>School of Chemical Engineering and Light Industry, Guangdong University of Technology, 510006, Guangzhou, P. R. China.

<sup>b</sup>Guangdong Provincial Laboratory of Chemistry and Fine Chemical Engineering Jieyang Center, Jieyang 515200, China

E-mail address: dehuahu@gdut.edu.cn (D. Hu) and smji@gdut.edu.cn (S. Ji)

## **1. Experimental Section**

### **1.1 General information**

All the reagents and solvents were purchased from commercial suppliers and used as received. The NMR spectra were recorded on a Bruker AVANCE 400 spectrometer, using tetramethylsilane (TMS) as the internal standard. Mass spectra (MS) were obtained on a Thermo Fisher TSQ Endura Mass spectrometer. Thermal gravimetric analysis (TGA) was measured on a NETZSCH STA449F5 Jupiter Synchronous thermal analyzer at a heating rate of 10 °C min<sup>-1</sup> under nitrogen flow rate of 80 mL min<sup>-1</sup>. Differential scanning calorimetry (DSC) was conducted on a METTLER TOLEDO (DSC3) unit at a heating rate of 10 °C min<sup>-1</sup> under nitrogen atmosphere. All ultraviolet–visible absorption spectra of the samples were recorded using Shimadzu UV-2700 UV-vis Spectrophotometer. The electrochemical properties were measured by cyclic voltammetry (CV) on PGSTAT 302N electrochemical workstation with a three electrode cell, Ag/AgNO<sub>3</sub> referenced against ferrocene/ferrocenium (Fc/Fc<sup>+</sup>), and glassy carbon electrode as working electrode at a scan rate of 0.1 V s<sup>-1</sup>, tetrabutylammonium hexafluorophosphate (Bu<sub>4</sub>NPF<sub>6</sub>) in anhydrous dichloromethane (0.1 M).

### **1.2 OLED fabrication**

OLEDs were fabricated on ITO-coated glass substrates with a sheet resistance of  $15 \Omega \text{ sq}^{-1}$  as a transparent anode, which were washed using detergent and underwent ultrasound bath of deionized water, acetone and isopropanol, successively for 15 minutes. And used after thoroughly dried and treated with  $\text{O}_2$  plasma for half of an hour. Under high vacuum better than  $10^{-6}$  Torr, materials were heated to sublimate and deposited onto ITO substrates. The rates of deposition were detected and controlled via quartz crystal oscillators, maintaining  $1\sim 2 \text{ \AA/s}$  for organic materials,  $0.1 \text{ \AA/s}$  for LiF and  $5 \text{ \AA/s}$  for aluminum cathode, respectively. Electroluminescence (EL) spectra and luminance were collected by a Spectroradiometer (Photo Research PR 650) and PMA-12 photonic multichannel analyzer (Hamamatsu), respectively. Current density and voltage were recorded on a Keithley 237 power source (Tektronix). External quantum efficiencies of devices were calculated using EL spectra and current, assuming the devices were Lambertian light sources.

## 2. Synthesis and Characterization

### Synthesis of 7-(anthracen-9-yl)-2,12-di-tert-butyl-5,9-dioxa-13b-boranaphtho[3,2,1-de]anthracene(BOOAn).

TDBA-Br (0.46 g, 1.0 mmol), B-An (0.33 g, 1.5 mmol, 1.5 equiv),  $\text{K}_2\text{CO}_3$  ( 2.56 g, 20.0 mmol), 5 mL distilled water, 20 mL toluene, 5 ml ethanol were placed in a 100 ml round-bottom flask. After the mixture was degassed,  $\text{Pd}(\text{PPh}_3)_4$  (58 mg, 0.05 mmol, 0.05 equiv) was added under nitrogen. The mixture was heated at  $90 \text{ }^\circ\text{C}$  for 24 hours under nitrogen.

The mixture was poured into water to quench the reaction and then extracted with dichloromethane. The organic phase was collected and dried over anhydrous Na<sub>2</sub>SO<sub>4</sub>. After evaporation of the solvent, the residue was purified via column chromatography by using petroleum ether/ dichloromethane (8:1, v/v) as eluent to afford yellow solid. (0.42 g, yield: 76%). <sup>1</sup>H NMR (500 MHz, CDCl<sub>3</sub>) δ 8.82 (d, J = 2.5 Hz, 2H), 8.55 (s, 1H), 8.07 (d, J = 8.5 Hz, 2H), 7.79 (dd, J = 8.7, 2.5 Hz, 2H), 7.73 (dd, J = 8.8, 1.2 Hz, 2H), 7.51 (s, 1H), 7.49 – 7.45 (m, 3H), 7.38 – 7.33 (m, 2H), 7.31 (s, 2H), 1.51 (s, 18H). <sup>13</sup>C NMR (126 MHz, CDCl<sub>3</sub>) δ 158.88, 157.57, 145.90, 145.19, 136.26, 131.66, 131.38, 130.39, 129.98, 128.43, 127.12, 126.82, 125.74, 125.31, 118.15, 111.54, 40.48, 32.71. LC-MS m/z: calcd for C<sub>40</sub>H<sub>35</sub>BO<sub>2</sub>, 558.5280; found, 559.28192 [M + H]<sup>+</sup>.

**Synthesis of 9,10-bis(2,12-di-tert-butyl-5,9-dioxa-13b-boranaphtho[3,2,1-de]anthracen-7-yl)anthracene(2BOOAn).**

TDBA-Br (1.012 g, 2.2 mmol, 2.2 equiv), 2B-An (0.43 g, 1.0 mmol), K<sub>2</sub>CO<sub>3</sub> ( 2.56 g, 20.0 mmol), 10 mL distilled water, 40 mL toluene, 10 ml ethanol were placed in a 100 ml round-bottom flask. After the mixture was degassed, Pd(PPh<sub>3</sub>)<sub>4</sub> (115.6 mg, 0.1 mmol, 0.1 equiv) was added under nitrogen. The mixture was heated at 100 °C for 24 hours under nitrogen. The mixture was poured into water to quench the reaction and then extracted with dichloromethane. The organic phase was collected and dried over anhydrous

Na<sub>2</sub>SO<sub>4</sub>. After evaporation of the solvent, the residue was purified via column chromatography by using petroleum ether/ dichloromethane (6:1, v/v) as eluent to afford yellow solid. (0.68 g, yield: 73%). <sup>1</sup>H NMR (400 MHz, CDCl<sub>3</sub>) δ 8.87 – 8.82 (d, J = 2.6 Hz, 4H), 7.86 – 7.77 (m, 8H), 7.57 – 7.51 (d, J = 8.7 Hz, 4H), 7.44 – 7.32 (m, 8H), 1.56 – 1.51 (s, 36H). <sup>13</sup>C NMR (126 MHz, CDCl<sub>3</sub>) δ 158.90, 157.62, 146.10, 145.21, 136.82, 131.71, 130.41, 129.59, 126.99, 125.53, 118.20, 111.65, 35.53, 31.69. HR-MS m/z: calcd for C<sub>66</sub>H<sub>60</sub>B<sub>2</sub>O<sub>4</sub>, 938.4678; found, 939.47614 [M + H]<sup>+</sup>.

**Table S1.** Crystal data and structure refinement of three compounds

Parameter	<b>BOOAn</b>	<b>2BOOAn</b>
Empirical formula	C <sub>40</sub> H <sub>35</sub> BO <sub>2</sub>	C <sub>33</sub> H <sub>30</sub> BO <sub>2</sub>
Formula weight	558.49	469.38
Temperature/K	150.00(10)	149.99(10)
Crystal system	triclinic	monoclinic
Space group	P-1	I2/a
a/Å	11.2801(3)	16.71187(12)
b/Å	11.4292(4)	11.15052(8)
c/Å	24.0256(7)	27.2171(2)
α/°	81.538(3)	90
β/°	89.599(2)	96.4401(7)
γ/°	78.204(3)	90

Volume/Å <sup>3</sup>	2998.17(16)	5039.79(7)
Z	4	8
$\rho_{\text{calc}}/\text{cm}^3$	1.237	1.237
$\mu/\text{mm}^{-1}$	0.569	0.577
F(000)	1184.0	1992.0
Crystal size/mm <sup>3</sup>	0.15 × 0.14 × 0.12	0.15 × 0.12 × 0.11
Radiation	Cu K $\alpha$ ( $\lambda = 1.54184$ )	Cu K $\alpha$ ( $\lambda = 1.54184$ )
2 $\Theta$ range for data collection/°	7.442 to 147.608	9.554 to 152.988
Index ranges	-14 ≤ h ≤ 11, -14 ≤ k ≤ 14, -29 ≤ l ≤ 29	-21 ≤ h ≤ 20, -13 ≤ k ≤ 13, -34 ≤ l ≤ 34
Reflections collected	21352	16787
Independent reflections	11769 [R <sub>int</sub> = 0.0383, R <sub>sigma</sub> = 0.0490]	5073 [R <sub>int</sub> = 0.0158, R <sub>sigma</sub> = 0.0116]
Data/restraints/parameters	11769/0/787	5073/0/331
Goodness-of-fit on F <sup>2</sup>	1.034	1.036
Final R indexes [I ≥ 2 $\sigma$ (I)]	R <sub>1</sub> = 0.0509, wR <sub>2</sub> = 0.1335	R <sub>1</sub> = 0.0411, wR <sub>2</sub> = 0.1079
Final R indexes [all data]	R <sub>1</sub> = 0.0587, wR <sub>2</sub> = 0.1422	R <sub>1</sub> = 0.0420, wR <sub>2</sub> = 0.1086
Largest diff. peak/hole / e Å <sup>-3</sup>	0.31/-0.34	0.24/-0.23

---

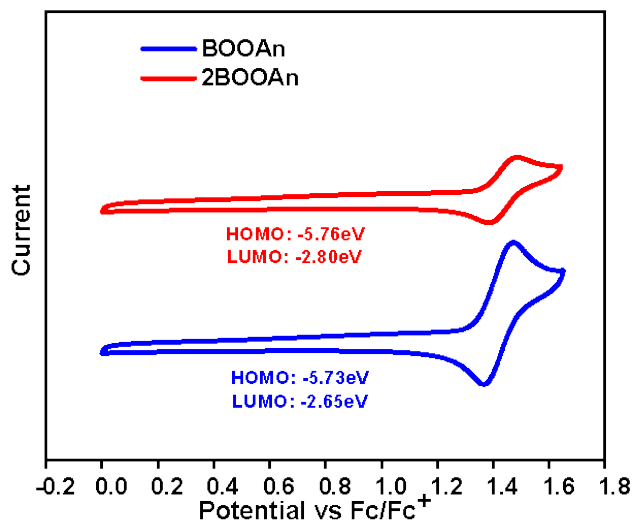


**Fig. S1.** CV of BOOAn and 2BOOAn, the potentials are calibrated against Fc/Fc<sup>+</sup> internal standard.

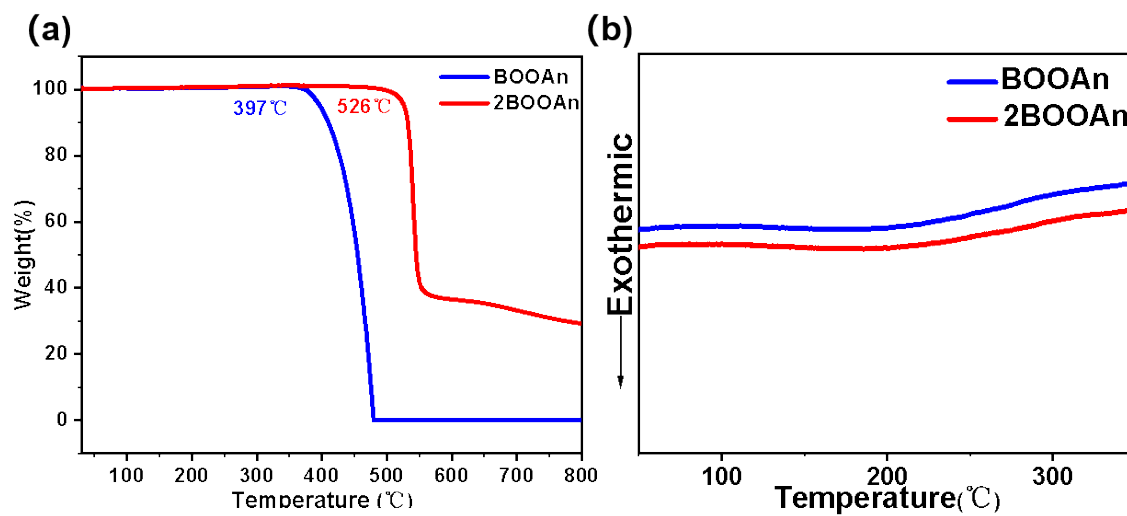


**Fig. S2.** TGA(a) and DSC (b) profiles of BOOAn and 2BOOAn.

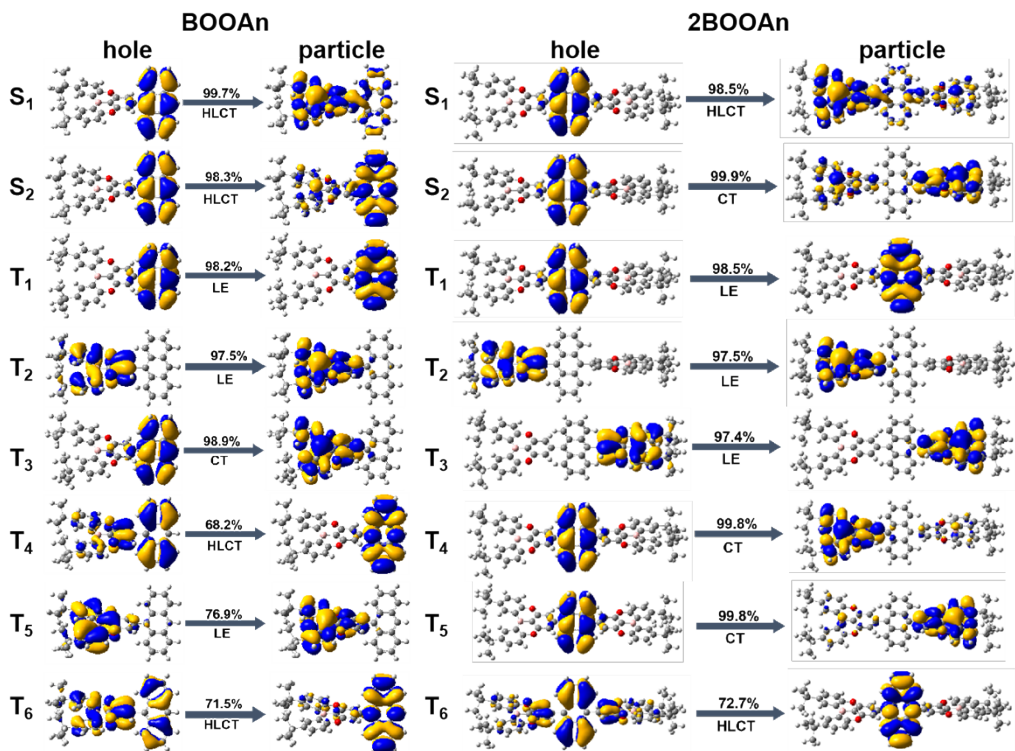


**Fig. S3.** The NTO transition character in first two singlet and six triplet states of BOOAn(a) and 2BOOAn(b).

**Table S2.** Detailed absorption and emission peak positions of BOOAn and 2BOOAn in different solvents.

Solvents	$\epsilon$	n	$f(\epsilon, n)$	BOOAn			2BOOAn		
				$\lambda_a$ (nm)	$\lambda_f$ (nm)	$\nu_a - \nu_f$ ( $\text{cm}^{-1}$ )	$\lambda_a$ (nm)	$\lambda_f$ (nm)	$\nu_a - \nu_f$ ( $\text{cm}^{-1}$ )
Hexane	0	1.375	0.0012	384	408	1532	383	435	3121
Toluene	2.38	1.494	0.014	386	420	2097	384	444	3519
Butylether	3.08	1.399	0.096	385	417	1993	382	440	3451



Ethyl ether	4.34	1.352	0.167	384	418	2118	381	437	3363
Ethyl acetate	6.02	1.372	0.2	382	433	3083	380	442	3691
Tetrahydrofuran	7.58	1.407	0.21	386	435	2918	381	445	3775
Dichloromethane	8.93	1.424	0.217	385	439	3195	381	446	3825
Acetonitrile	37.5	1.344	0.305	387	470	4536	377	456	4595

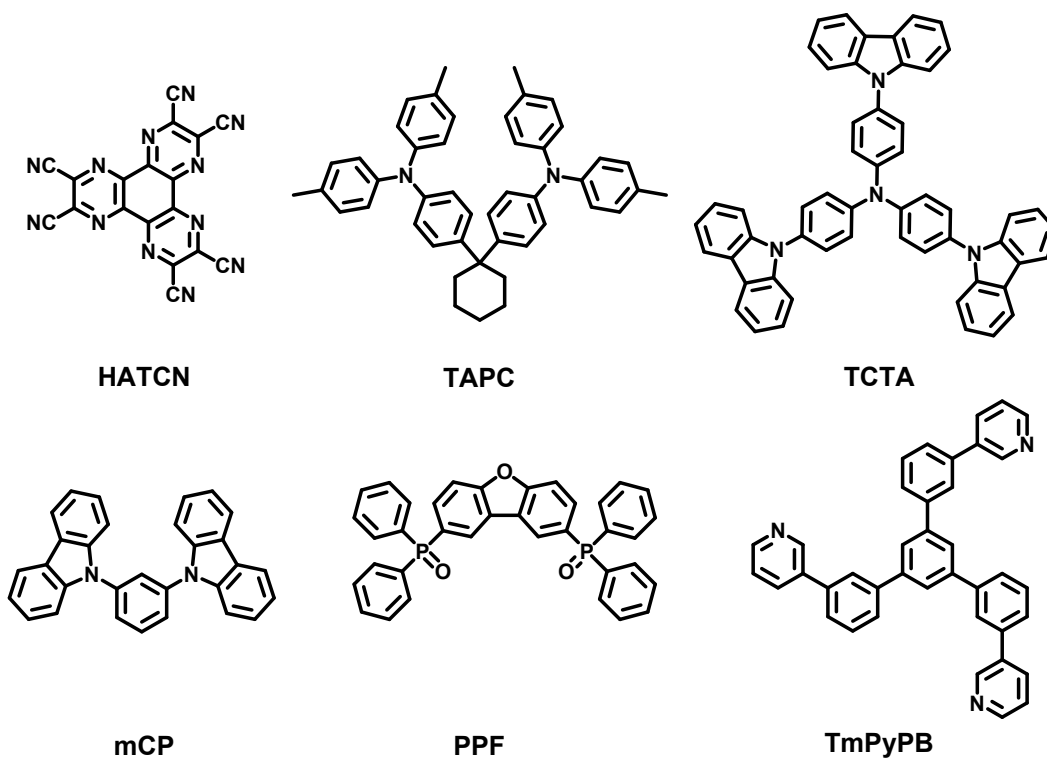


**Fig. S4.** Chemical structures of the OLED materials.

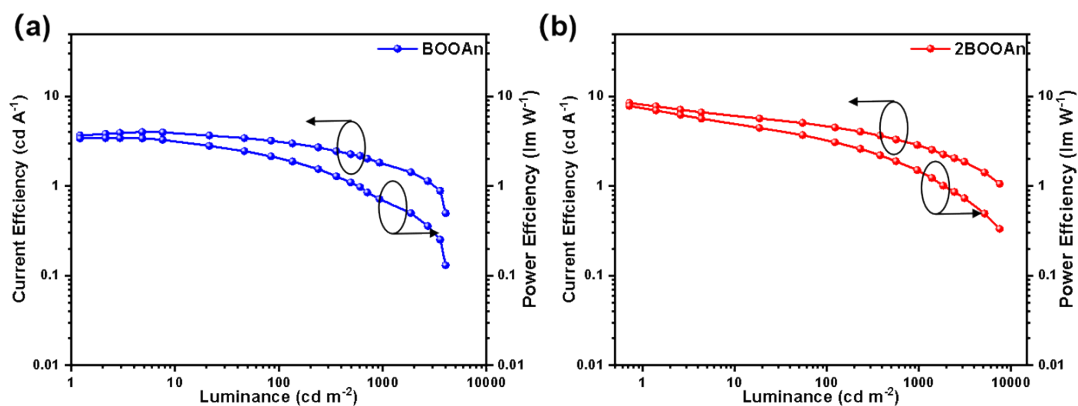


**Fig. S5.** CE and PE as a function of luminance for doped devices based on (a) BOOAn and (b) 2BOOAn.

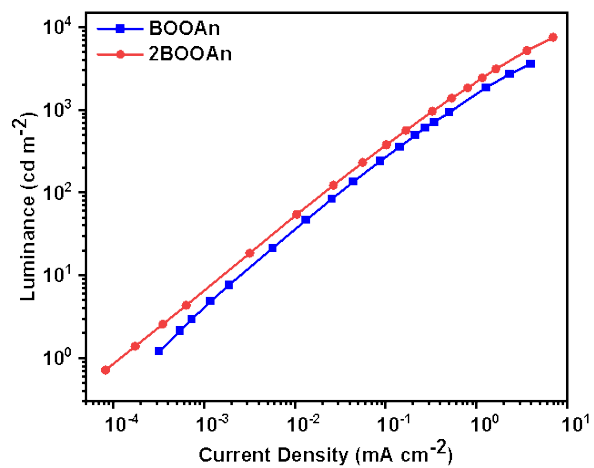


**Fig. S6.** Luminescence-current density curves of the doped devices BOOAn and 2BOOAn.

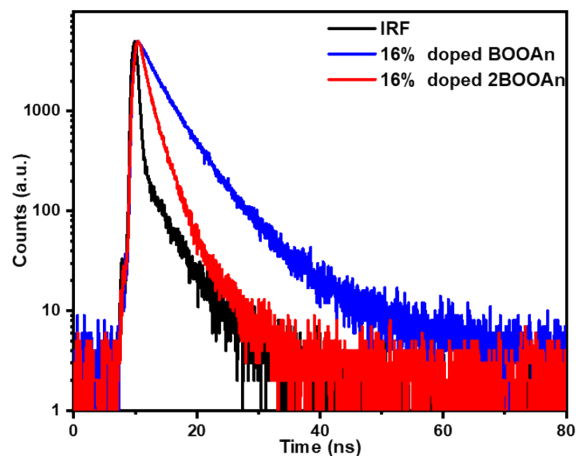


**Fig. S7.** The transient PL decay of BOOAn and 2BOOAn in doped film.

**Table S3.** The kinetic parameters of BOOAn and 2BOOAn.

compound	$\tau_1^a$	$\tau_2^b$	$\Phi^c$	$\Phi_{PF}^d$	$\Phi_{DF}^e$	$K_r^f$	$K_{nr}^g$	$k_{ISC}^h$	$k_{RISC}^i$
	(ns)	(ns)	(%)	(%)	(%)	(s <sup>-1</sup> )	(s <sup>-1</sup> )	(s <sup>-1</sup> )	(s <sup>-1</sup> )
BOOAn	3.4	7.8	67	48.2	18.8	$1.66 \times 10^8$	$0.82 \times 10^8$	$0.47 \times 10^8$	$3.16 \times 10^8$
2BOOAn	1.3	3.4	74	49.2	24.8	$4.51 \times 10^8$	$1.59 \times 10^8$	$1.59 \times 10^8$	$7.16 \times 10^8$

<sup>a</sup>Prompt fluorescence lifetime; <sup>b</sup>delayed fluorescence lifetime; <sup>c</sup>fluorescent quantum yield of doped film; <sup>d</sup>prompt fluorescent quantum yield of doped film; <sup>e</sup>delayed fluorescent quantum yield of doped film; <sup>f</sup>rate of radiative transition ( $k_r = \Phi_{PF}/\tau_1 + \Phi_{PF}/\tau_2$ ); <sup>g</sup>rate of non-radiative transition ( $k_{nr} = k_r(1-\Phi)/\Phi$ ); <sup>h</sup>rate of intersystem crossing ( $K_{ISC} = 1/\tau_1 - 1/\tau_2 - k_{nr}$ ); <sup>i</sup>rate of reverse intersystem crossing ( $k_{RISC} = \Phi_{DF}/(k_{ISC}\Phi_{PF}\tau_1\tau_2)$ ).

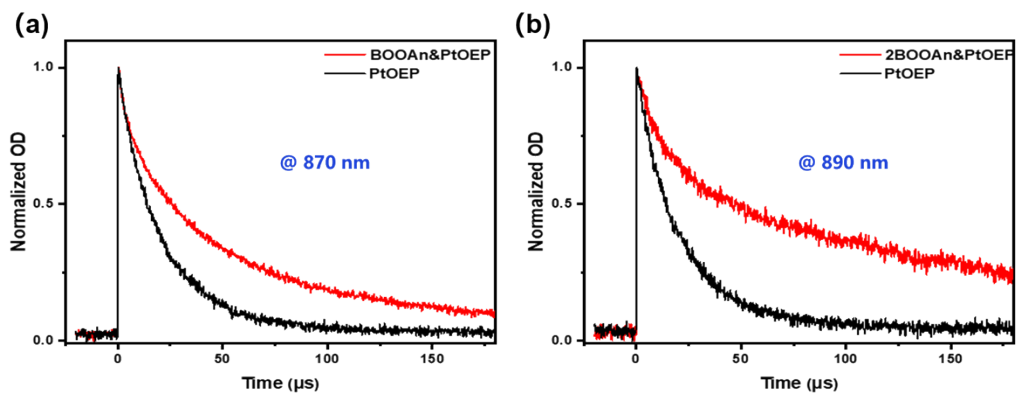


**Fig. S8.** Triplet decay trace detected at (a) 870 nm and (b) 890 nm.

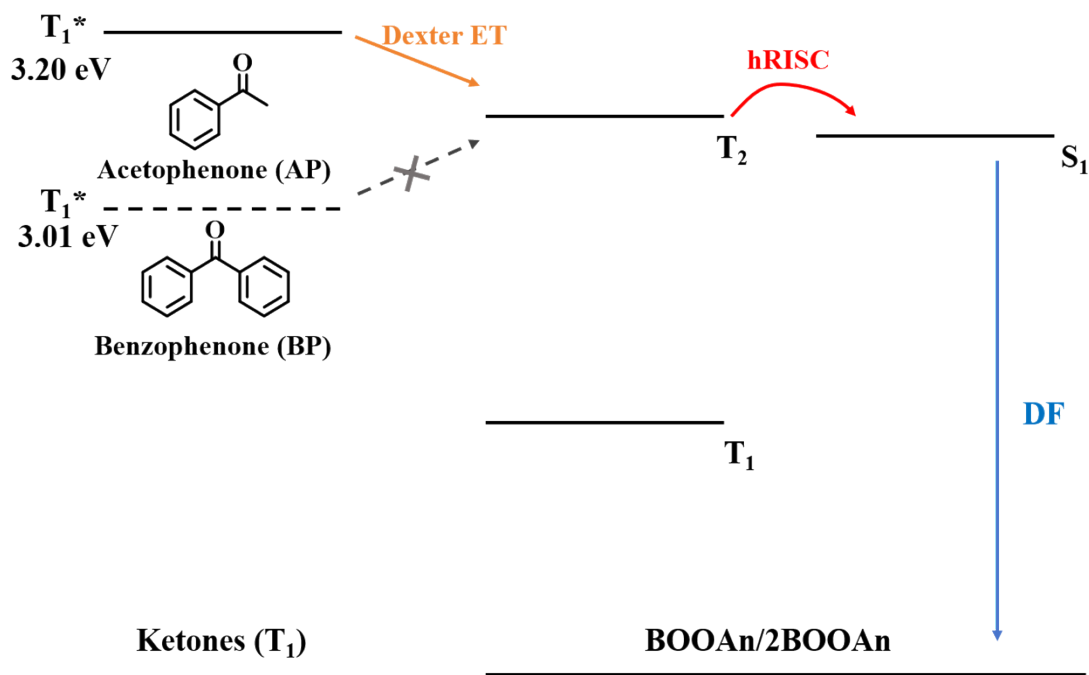


**Fig. S9.** Schematic illustration of the excited states of the ketones and BOOAn/2BOOAn and the corresponding photophysical processes.

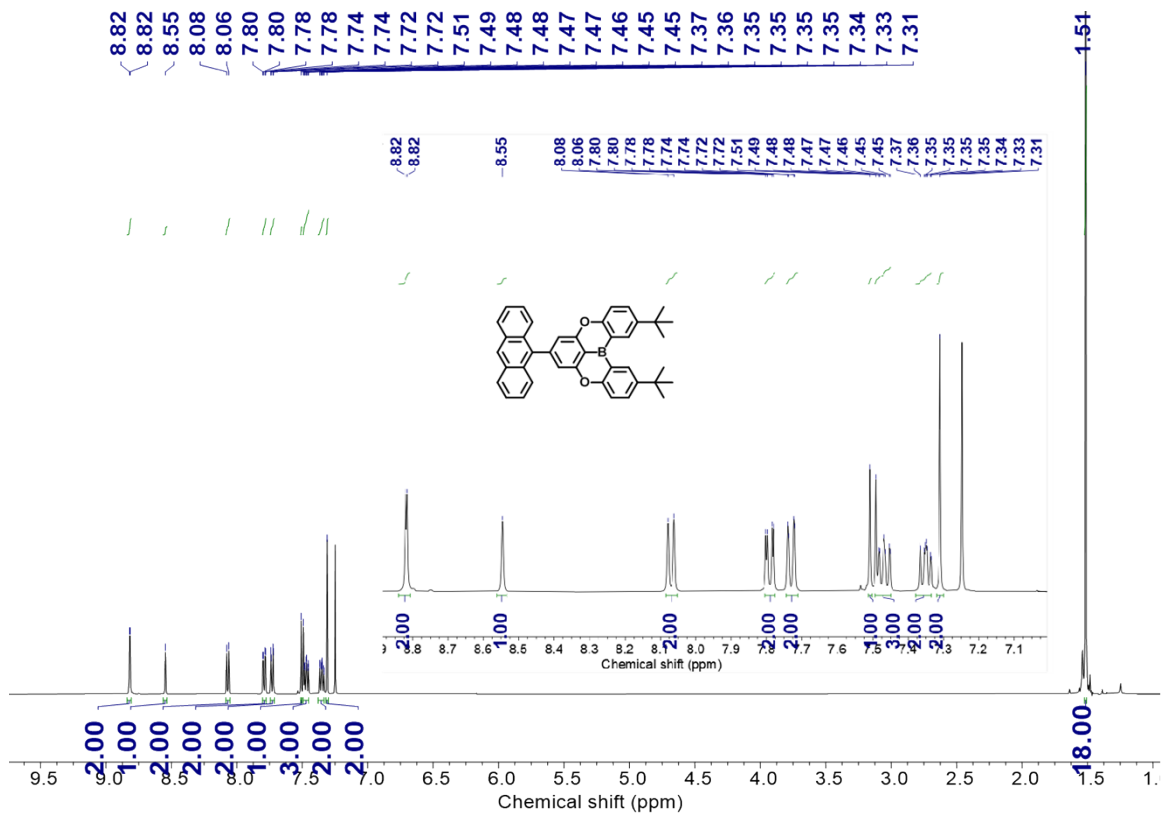


**Fig. S10.**  $^1\text{H}$  NMR of BOOAn ( $\text{CDCl}_3$ ).

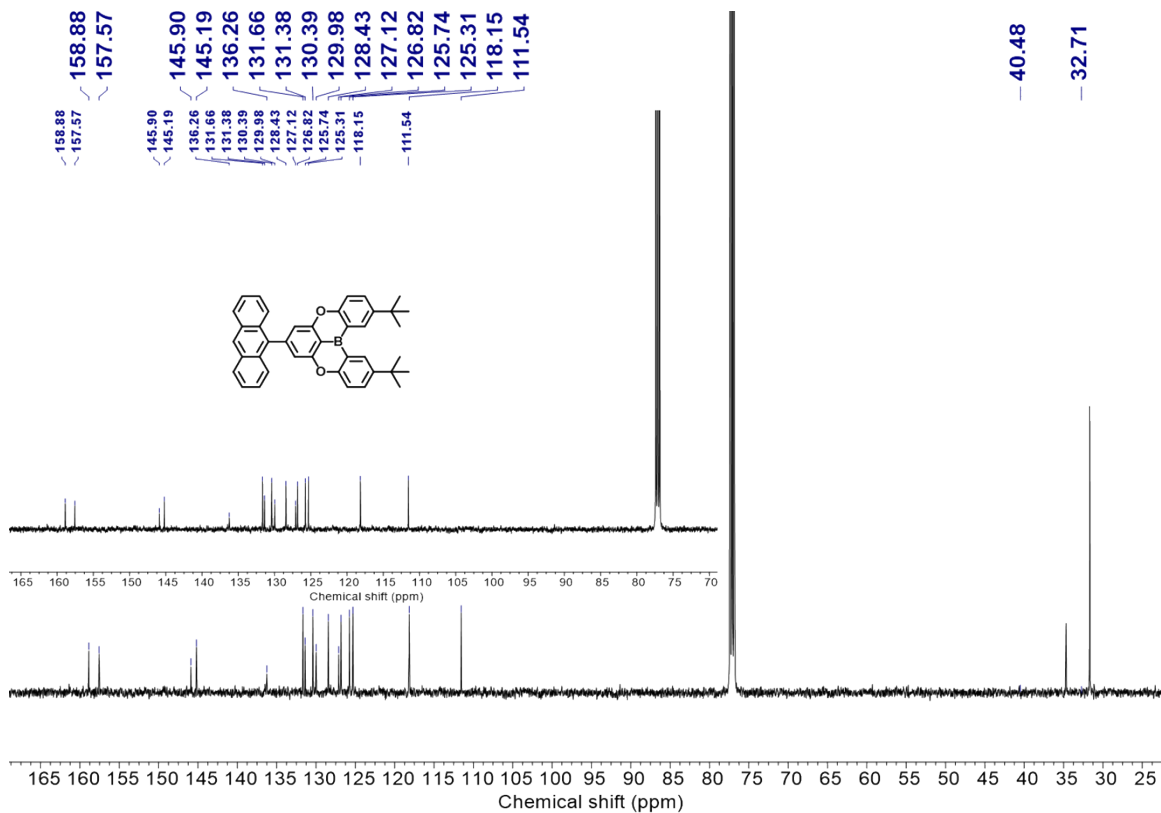


**Fig. S11.** <sup>13</sup>C NMR of BOOAn (CDCl<sub>3</sub>).

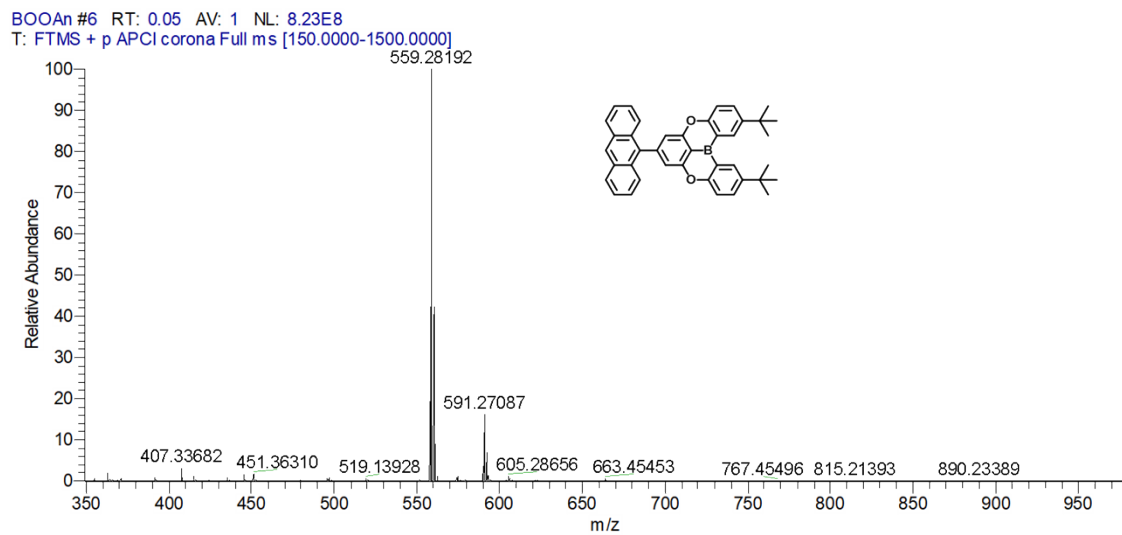


**Fig. S12.** HR MS of BOOAn.

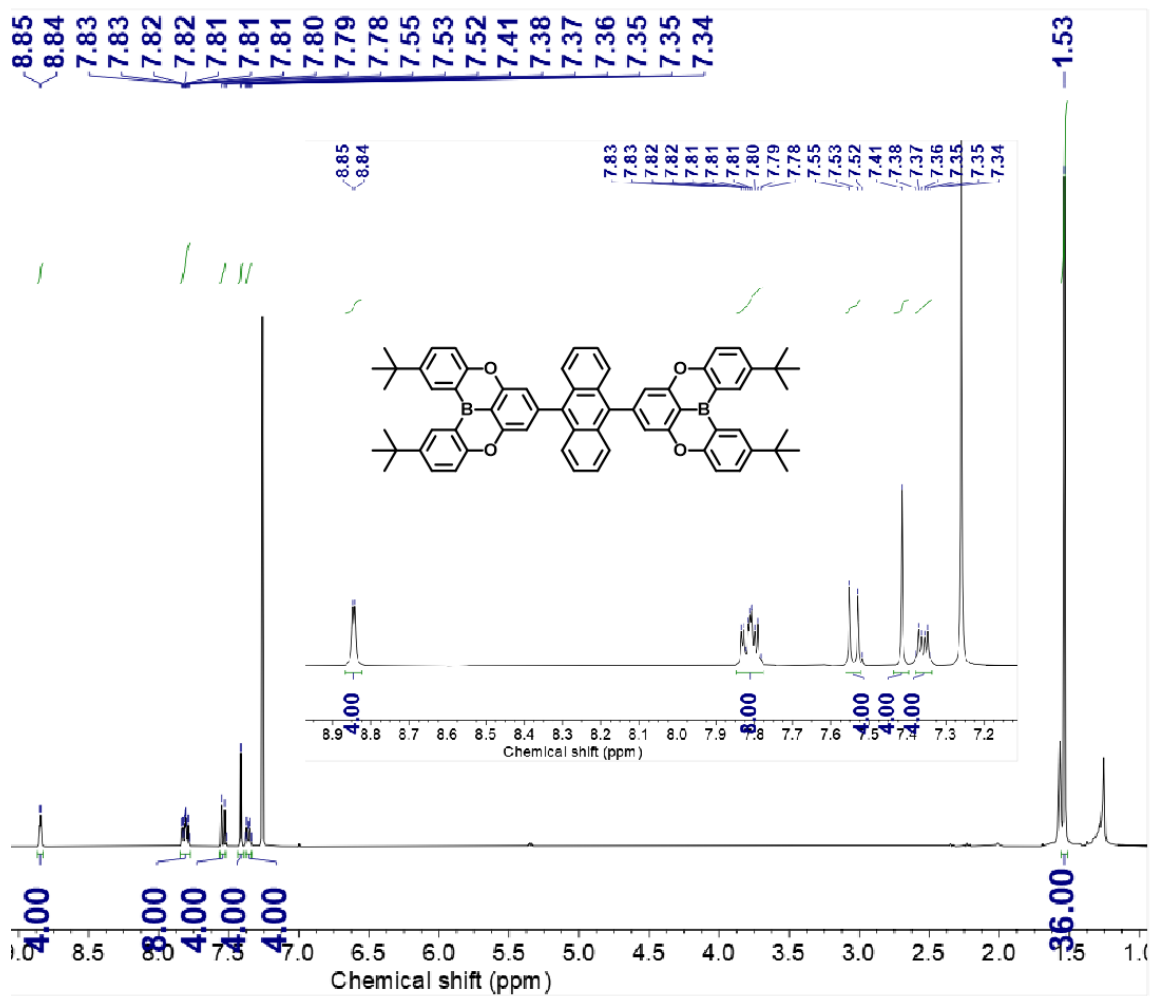


Fig. S13.  $^1\text{H}$  NMR of 2BBOAn ( $\text{CDCl}_3$ ).

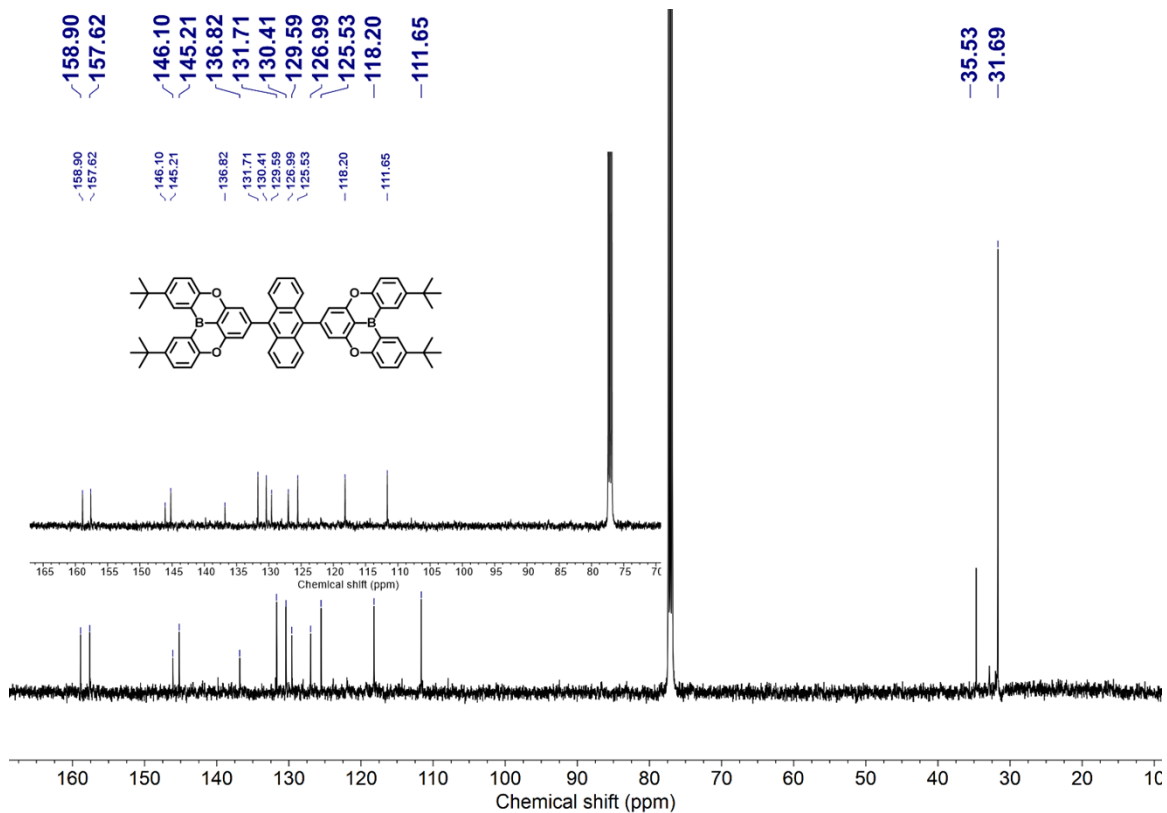


Fig. S14.  $^{13}\text{C}$  NMR of 2BOOAn ( $\text{CDCl}_3$ ).

2BOOAn #6 RT: 0.06 AV: 1 SB: 1 0.02 NL: 9.27E6  
 T: FTMS + p APCI corona Full ms [150.0000-1500.0000]

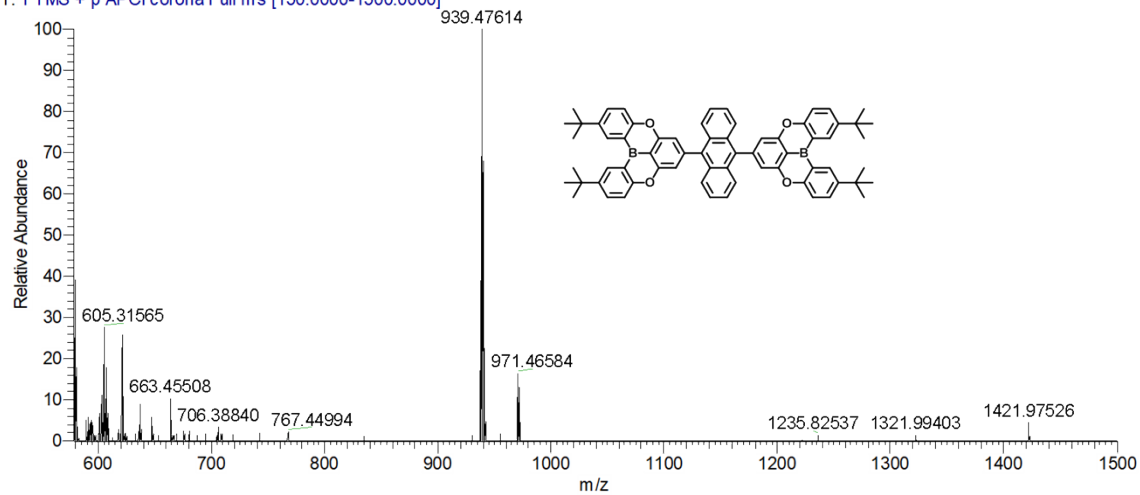


Fig. S15. HR MS of 2BOOAn.